PHYSICAL REVIEW D **78,** 054008 (2008)

Deciphering top flavor violation at the CERN LHC with *B* factories

Patrick J. Fox,[1] Zoltan Ligeti,[1] Michele Papucci,[1,2] Gilad Perez,[3] and Matthew D. Schwartz[4]

[1]*Ernest Orlando Lawrence Berkeley National Laboratory, University of California, Berkeley, California 94720, USA*
[2]*Department of Physics, University of California, Berkeley, California 94720, USA*
[3]*C.N. Yang Institute for Theoretical Physics, State University of New York, Stony Brook, New York 11794-3840, USA*
[4]*Department of Physics and Astronomy, Johns Hopkins University, 3400 North Charles Street, Baltimore, Maryland 21218, USA*

(Received 25 April 2007; published 11 September 2008)

The CERN LHC will have unprecedented sensitivity to flavor-changing neutral current (FCNC) top quark decays, whose observation would be a clear sign of physics beyond the standard model. Although many details of top flavor violation are model dependent, the standard model gauge symmetries relate top FCNCs to other processes, which are strongly constrained by existing data. We study these constraints in a model-independent way, using a low energy effective theory from which the new physics is integrated out. We consider the most important operators which contribute to top FCNCs and analyze the current constraints on them. We find that the data rule out top FCNCs at a level observable at the LHC due to most of the operators comprising left-handed first or second generation quark fields, while there remains a substantial window for top decays mediated by operators with right-handed charm or up quarks. If FCNC top decays are observed at the LHC, such an analysis may help decipher the underlying physics.

DOI: 10.1103/PhysRevD.78.054008 PACS numbers: 14.65.Ha

I. INTRODUCTION

The CERN Large Hadron Collider (LHC) will have unprecedented sensitivity to flavor-changing neutral currents (FCNCs) involving the top quark, such as $t \to cZ$. With a $t\bar{t}$ pair production cross section of about 800 pb and after 100 fb^{-1} of integrated luminosity, the LHC will explore branching ratios down to the 10^{-5} level [1,2]. Flavor-changing neutral currents are highly suppressed in the standard model (SM), but are expected to be enhanced in many models of new physics (NP). Because top FCNCs are clean signals, they are a good place to explore new physics. There are important constraints from *B* physics on what top decays are allowed, and understanding these constraints may help decipher such an FCNC signal. In this paper, we calculate the dominant constraints on top FCNCs from low energy physics and relate them to the expected LHC reach using a model-independent effective field theory description.

Flavor physics involving only the first two generations is already highly constrained, but the third generation could still be significantly affected. Of course, the new flavor physics could be so suppressed that it will not be observable at all at the LHC. However, since the stabilization of the Higgs mass is expected to involve new physics to cancel the top loop, it is natural to expect some new flavor structure which may show up in the top quark couplings to other standard model fields. Thus, one may expect flavor physics to be related to the electroweak scale, and then flavor-changing effects involving the top quark are a natural consequence.

Although there are many models which produce top FCNCs, the low energy constraints are independent of the details of these models. The new physics can be integrated out, leaving a handful of operators relevant at the weak scale involving only standard model fields. These operators mediate both FCNC top decays and flavor-changing transitions involving lighter quarks. Thus, the two can be related without reference to a particular model of new physics, provided there is no additional NP contributing to the *B* sector. The low energy constraints can be applied to any model in which top FCNCs are generated, and the constraints on the operators may give information on the scale at which the physics that generates them should appear.

Analyses of FCNC top decays have been carried out both in the context of specific models [3] and using model-independent approaches [4]. However, in most cases the effective Lagrangian analyzed involved the SM fields after electroweak symmetry breaking. As we shall see, the scale Λ at which the operators responsible for top FCNC are generated has to be above the scale v of electroweak symmetry breaking. Thus, integrating out the new physics should be done before electroweak symmetry breaking, leading to an operator product expansion in v/Λ. The requirement of $SU(2)_L$ invariance provides additional structure on the effective operators [5], which helps constrain the expectations for top FCNCs. For example, an operator involving the left-handed (t, b) doublet, the $SU(2)$ gauge field, and the right-handed charm quark can lead to $b \to s\gamma$ at one loop, but also directly to a $b \to c$ transition. If we ignored $SU(2)_L$ invariance, we would only have the $b \to s\gamma$ constraint, and the resulting bound would be different. An important feature of our analysis is that, after electroweak symmetry breaking, the resulting operators can modify even SM parameters which contribute at tree level to *B* physics observables, such as $|V_{cb}|$.

The organization of this paper is as follows. In Sec. II we introduce the effective Lagrangian relevant for top FCNCs.

We also explain why some operators can be neglected and introduce conventions used throughout the paper. In Sec. III we calculate how these operators affect top quark decays and integrate out the W and Z bosons and the top quark to match onto the relevant effective theory at the weak scale. In Sec. IV we relate the experimental constraints to the Wilson coefficients calculated in Sec. III, focusing mostly on observables related to B physics. This leads directly to predictions for the top branching ratio. Section V contains a summary of the results and our conclusions. We include an appendix with details of the calculations.

II. EFFECTIVE LAGRANGIAN FOR TOP FCNC

We consider an effective Lagrangian

$$\mathcal{L}_{\text{eff}} = \frac{1}{\Lambda^2}\sum (C_i O_i + C_i' O_i'), \tag{1}$$

where the O_i operators involve third and second generation quarks and the O_i' involve the third and first generations. Since we are interested in top quark decays, we define O_i and O_i' in the mass basis for the up-type quarks.

A complete set of dimension-six operators which give a tcZ or $tc\gamma$ vertex are

$$\begin{aligned}
O_{LL}^{u} &= i[\bar{Q}_3\tilde{H}][(\not{D}\tilde{H})^\dagger Q_2] - i[\bar{Q}_3(\not{D}\tilde{H})][\tilde{H}^\dagger Q_2] + \text{H.c.},\\
O_{LL}^{h} &= i[\bar{Q}_3\gamma^\mu Q_2][H^\dagger \overleftrightarrow{D}_\mu H] + \text{H.c.},\\
O_{RL}^{w} &= g_2[\bar{Q}_2\sigma^{\mu\nu}\sigma^a\tilde{H}]t_R W_{\mu\nu}^a + \text{H.c.},\\
O_{RL}^{b} &= g_1[\bar{Q}_2\sigma^{\mu\nu}\tilde{H}]t_R B_{\mu\nu} + \text{H.c.},\\
O_{LR}^{w} &= g_2[\bar{Q}_3\sigma^{\mu\nu}\sigma^a\tilde{H}]c_R W_{\mu\nu}^a + \text{H.c.},\\
O_{LR}^{b} &= g_1[\bar{Q}_3\sigma^{\mu\nu}\tilde{H}]c_R B_{\mu\nu} + \text{H.c.},\\
O_{RR}^{u} &= i\bar{t}_R\gamma^\mu c_R[H^\dagger \overleftrightarrow{D}_\mu H] + \text{H.c.}
\end{aligned} \tag{2}$$

The brackets mean contraction of $SU(2)$ indices, Q_3 and Q_2 are the left-handed $SU(2)$ doublets for the third and second generations, t_R and c_R are the right-handed $SU(2)$ singlets for the top and charm quarks, H is the SM Higgs doublet, $\tilde{H} = i\sigma_2 H^*$, and the index a runs over the $SU(2)$ generators. The first lower L or R index on the operators denotes the $SU(2)$ representation of the third generation quark field, while the second lower index refers to the representation of the first or second generation field. In this basis all of the derivatives act on the Higgs fields. We could also consider operators directly involving gluons, but since the indirect constraints on gluonic currents are very weak (see, e.g., [6]), we restrict our focus to the electroweak operators in Eq. (2). The forms of the operators in Eq. (2) after electroweak symmetry breaking are given in the Appendix.

Throughout the paper we focus on those new operators that contribute to $t \to cZ, c\gamma$. In any particular model there may be additional contributions to Eq. (1) that contribute to $\Delta F = 1$ and $\Delta F = 2$ processes in the down sector (e.g., four-fermion operators). These operators have suppressed contributions to top FCNCs. When we bound the coefficients of the operators in Eq. (2) from B physics, we neglect these other contributions. In any particular model these two sets of operators may have related coefficients. Unless there are cancellations between the different operators, the bounds will not get significantly weaker.

There are other dimension-six operators that can mediate FCNC top decays (for example, $\bar{t}_R\gamma^\mu D^\nu c_R B_{\mu\nu}$). But these can always be reduced to a linear combination of the operators included in Eq. (2) plus additional four-fermion operators and operators involving $Q_L q_R HHH$ fields. For instance, operators involving two quark fields and three covariant derivatives can be written in terms of operators involving fewer derivatives using the equations of motion. Operators involving two quark fields and two covariant derivatives (e.g., $\bar{Q}_3 D_\mu c_R D^\mu \tilde{H}$) can be written in terms of operators involving the commutator of derivatives included in Eq. (2) plus operators with one derivative and four-fermion operators. Finally, operators involving two quark fields and one covariant derivative can be written in a way that the derivative acts on the H field, as in Eq. (2), plus four-fermion operators.

Of the four-fermion operators which appear after the reduction of the operator basis, some are suppressed by small Yukawa couplings and can simply be neglected. However, some are not suppressed, and of those, the biggest concern would be semileptonic four-fermion operators, like $(\bar{t}c)(\bar{\ell}\ell)$. These contribute to the same final state as $t \to cZ \to c\ell^+\ell^-$. (We emphasize $Z \to \ell^+\ell^-$, because the LHC is expected to have the best sensitivity in this channel [1,2].) However, the invariant mass of the $\ell^+\ell^-$ pair coming from a four-fermion operator will have a smooth distribution and not peak around m_Z, so the Z-mediated contribution can be disentangled experimentally. Operators with $(\bar{t}c)(\bar{q}q)$ flavor structure also contribute to $t \to c\ell^+\ell^-$ or $t \to c\gamma$ at one loop, but their contributions are suppressed by $\alpha/(4\pi)$. Finally, operators with the $Q_L q_R HHH$ structure either renormalize Yukawa couplings, or contribute to FCNCs involving the Higgs (e.g., $t \to ch$), but we do not consider such processes, as explained later.

Throughout most of this paper we consider each of the operators one at a time and constrain their coefficients. This is reasonable as the operators do not mix under renormalization. One exception is that O_{LL}^u and O_{LL}^h mix with one another between the scales Λ and v, so it would be unnatural to treat them independently. Their mixing is given by

$$\frac{\mathrm{d}}{\mathrm{d}\ln\mu}\begin{pmatrix} C_{LL}^u(\mu) \\ C_{LL}^h(\mu) \end{pmatrix} = \frac{3\alpha_2}{8\pi}\begin{pmatrix} 5 & 0 \\ -4 & 1 \end{pmatrix}\begin{pmatrix} C_{LL}^u(\mu) \\ C_{LL}^h(\mu) \end{pmatrix}, \tag{3}$$

where $\alpha_2 = \alpha/\sin^2\theta_W$ is the $SU(2)$ coupling. [The zero in the anomalous dimension matrix is due to the fact that the

custodial $SU(2)$ preserving operator O^h_{LL} cannot mix into the custodial $SU(2)$ violating O^u_{LL}]. So, we will also carry out a combined analysis for these two operators.

We have written the operators in Eq. (2) in terms of a single SM Higgs doublet. In principle, there may be many new Higgs scalars, but only those that acquire a vacuum expectation value (vev) will contribute to $t \to cZ$ and $c\gamma$. Since a triplet Higgs vev is tightly constrained by electroweak precision tests, we concentrate on the possibility of multiple Higgs doublets. With the introduction of extra Higgs doublets, there are more operators of each particular type (O^u_{LL}, O^h_{LL}, etc.), one linear combination of which gives rise to $t \to cZ$ and $c\gamma$. There are also several physical Higgs states that can contribute in loops in low energy processes. For each type of operator, a different linear combination of couplings enters in low energy measurements. However, without cancellations this will only differ from the one Higgs case by a number of order one. This allows our results to be applied to the general case of multiple Higgs doublets.[1] Of course, the Higgs sector is also relevant to FCNCs involving the Higgs, such as $t \to ch$, but we do not consider such processes as they are more model dependent.

Once we go beyond models with minimal flavor violation (MFV) [7], the possibility of new CP violating phases in the NP should be considered. In MFV models, top FCNC is not observable at the LHC. In models such as next-to-minimal flavor violation (NMFV) [8], top FCNCs could be observable and the Wilson coefficients can be complex. It is not always the case that the constraints are weaker when the NP Wilson coefficients are real (in the basis where the up-type Yukawa matrix is real and diagonal). Rather, interference patterns realized in some of the observables mean the constraints are weakest when some of the new phases are different from 0 or π. We shall point out the places where phases associated with the new operators can play an important role and how we treat them.

In addition to the B physics related constraints we will derive in this paper, one can also use constraints from electroweak precision observables. However, these strongly bound flavor-diagonal operators whereas the flavor nondiagonal operators in Eq. (2), which contribute to top FCNCs, are far less constrained. For instance, the O^u_{LL} operator corrects the W propagator at one loop and so contributes to the T parameter. The loops involve a t or c quark, and have one insertion of O^u_{LL} and one insertion of V_{ts} or V_{cb}. Thus, the contribution is suppressed by $|V_{ts}| \sim |V_{cb}| \sim 0.04$ relative to an insertion of the flavor-diagonal equivalent of O^u_{LL}, $\bar{Q}_3 \tilde{H} \not{\partial} \tilde{H}^\dagger Q_3$. In contrast, when considering low energy FCNC processes, O^u_{LL} will be more strongly constrained than its flavor-diagonal version. That is, flavor-diagonal operators are more tightly constrained by electroweak observables than by low energy FCNCs, while the off-diagonal operators are more tightly constrained by low energy FCNCs. Moreover, the mixing between these two classes of operators is small. It occurs at one loop proportional to $y_b^2 |V_{cb}|$, where the factor of y_b, the bottom Yukawa coupling, is due to a Glashow-Iliopoulos-Maiani mechanism. Thus, we can think of the flavor-diagonal and off-diagonal operators as independent. And so for the purpose of studying top FCNCs, we are justified in neglecting flavor-diagonal operators and the relatively weak constraints from electroweak precision tests.

[1]One possible exception is if an extended Higgs sector allows Yukawa couplings larger than in the SM, for example, in a two Higgs doublet model at large $\tan\beta$. Then a Higgs loop may give additional unsuppressed contributions when we match to the Wilson coefficients at the electroweak scale.

III. WEAK SCALE MATCHING

In this section we derive how the NP operators modify flavor-changing interactions at the electroweak scale and derive the effective Hamiltonian in which the t, W, and Z are integrated out. For numerical calculations we use, besides the Higgs vev, $v = 174.1$ GeV and other standard PDG values [9], $|V_{ts}| = 41.0 \times 10^{-3}$ [10], and $m_t = 171$ GeV [11].

A. Top quark decays

After electroweak symmetry is broken, the operators in Eq. (2) give rise to $t \to cZ$ and $t \to c\gamma$ FCNC decays. The analytic expressions for the partial widths of these decays are given in Eq. (A2) in the Appendix. Numerically, the $t \to cZ$ branching ratio in terms of the Wilson coefficients is

$$\begin{aligned}\mathcal{B}(t \to cZ) = \left(\frac{1\ \text{TeV}}{\Lambda}\right)^4 \times 10^{-4} \times \{&1.4[|C^b_{LR}|^2 + |C^b_{RL}|^2] \\ &- 9.6\,\text{Re}(C^b_{LR} C^{w*}_{LR} + C^b_{RL} C^{w*}_{RL}) \\ &+ 16[|C^w_{LR}|^2 + |C^w_{RL}|^2] \\ &- 8.3\,\text{Re}[(C^h_{LL} + C^u_{LL}) C^{b*}_{RL} - C^b_{LR} C^{u*}_{RR}] \\ &+ 28\,\text{Re}[(C^h_{LL} + C^u_{LL}) C^{w*}_{RL} - C^w_{LR} C^{u*}_{RR}] \\ &+ 17[|C^h_{LL} + C^u_{LL}|^2 + |C^u_{RR}|^2]\}. \end{aligned} \quad (4)$$

The $tc\gamma$ vertex, which has a magnetic dipole structure as required by gauge invariance, is induced only by the left-right operators. The branching ratio for $t \to c\gamma$ is

$$\begin{aligned}\mathcal{B}(t \to c\gamma) = \left(\frac{1\ \text{TeV}}{\Lambda}\right)^4 \times 10^{-4} \times 8.2[&|C^b_{LR} + C^w_{LR}|^2 \\ &+ |C^b_{RL} + C^w_{RL}|^2]. \end{aligned} \quad (5)$$

The analogous expressions for $t \to u$ decays are obtained by replacing C_i by C'_i in Eqs. (4) and (5).

The LHC will have unparalleled sensitivity to such decays. With 100 fb^{-1} data, the LHC will be sensitive (at 95% CL) to branching ratios of 5.5×10^{-5} in the $t \to cZ$ channel and 1.2×10^{-5} in the $t \to c\gamma$ channel [1]. In the

SM, $\mathcal{B}(t \to cZ, c\gamma)$ are of order $\alpha(V_{cb}\alpha m_b^2/m_W^2)^2 \sim 10^{-13}$, so an experimental observation would be a clear sign of new physics. Equations (4) and (5) will allow one to translate the measurements or upper bounds on these branching ratios to the scale of the individual operators.

B. B decays

Many of the operators in Eq. (2) modify SM interactions at tree level (this possibility was discussed in [5]). After electroweak symmetry breaking, O^u_{LL} gives rise to a $\bar{b}Wc$ vertex with the same Dirac structure as the SM, so the measured value of V_{cb} (which we denote $V_{cb}^{\rm exp}$) will be the sum of the two. This allows us to absorb the new physics contribution of C^u_{LL} into the known value of $V_{cb}^{\rm exp}$—in processes where V_{cb} and C^u_{LL} enter in the same way, the dependence on C^u_{LL} cannot be disentangled. For example, the SM unitarity condition, $V^*_{tb}V_{td} + V^*_{cb}V_{cd} + V^*_{ub}V_{ud} = 0$, would be violated if one simply shifted the SM values by the NP contributions. However, the Cabibbo-Kobayashi-Maskawa (CKM) fits have unitarity built in, so the NP contribution to V_{cb} causes a shift in the values of V_{ts} and V_{td} extracted from the CKM fit, $V_{ts}^{\rm fit}$ and $V_{td}^{\rm fit}$. Since we cannot measure all CKM elements independently, we have to replace V_{ts} and V_{td} by $V_{ts}^{\rm fit}$ and $V_{td}^{\rm fit}$, plus modified NP contributions. (Recall that V_{ts} and V_{td} are only constrained from loop processes where they enter together with new physics contributions.) With these redefinitions we can use $V_{cb}^{\rm exp}$, $V_{ts}^{\rm fit}$, and $V_{td}^{\rm fit}$ in the CKM fit, and the NP will only have distinguishable effects in SM loop processes. An analogous procedure applies to the $t \to u$ contribution to $V_{ub}^{\rm exp}$, $V_{td}^{\rm fit}$, and $V_{ts}^{\rm fit}$. Some other operators such as C^w_{LR} do not generate a $\bar{b}Wc$ vertex with the same Dirac structure as the SM. Thus, their contributions to observables from which V_{cb} is extracted may be disentangled as discussed in the following.

At leading order in the Wolfenstein parameter (Cabibbo angle), λ, these relations are

$$\begin{aligned} V_{cb} &= V_{cb}^{\rm exp} + (v^2/\Lambda^2)C^u_{LL}V_{tb}, \\ V_{ub} &= V_{ub}^{\rm exp} + (v^2/\Lambda^2)C'^u_{LL}V_{tb}, \\ V^*_{ts} &= V_{ts}^{*\rm fit} - (v^2/\Lambda^2)(C^u_{LL}V^*_{cs} + C'^u_{LL}V^*_{us}), \\ V^*_{td} &= V_{td}^{*\rm fit} - (v^2/\Lambda^2)(C^u_{LL}V^*_{cd} + C'^u_{LL}V^*_{ud}). \end{aligned} \tag{6}$$

The O^w_{LR} (O'^w_{LR}) also modifies the $\bar{b}Wc$ ($\bar{b}Wu$) vertex, but with different Dirac structure from the SM, so its effects can be separated from the SM contribution. Finally, O^h_{LL} (O'^h_{LL}) gives tree-level FCNC, since it contains a $\bar{b}Zs$ ($\bar{b}Zd$) interaction.

At the one-loop level, the operators in Eq. (2) contribute to $b \to s$ transitions. The constraints from B physics are easiest to analyze by matching these operators onto operators containing only the light SM fields at a scale $\mu \sim m_W$. We use the standard basis as defined in [12]. Integrating out the top, W, and Z, the most important operators for $B \to X_s\gamma$ and $B \to X_s\ell^+\ell^-$ which are affected by NP are

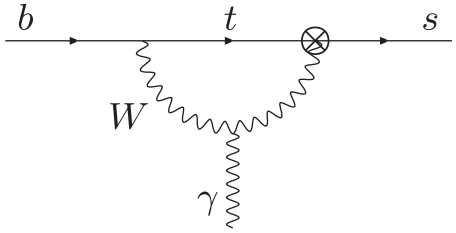

FIG. 1. A one-loop contribution from O^w_{RL} (denoted by ⊗) to $O_{7\gamma}$.

$$\begin{aligned} O_{7\gamma} &= \frac{e}{8\pi^2}[m_b\bar{s}\sigma^{\mu\nu}(1+\gamma_5)b]F_{\mu\nu}, \\ O_{9V} &= [\bar{s}\gamma^\mu(1-\gamma_5)b][\bar{\ell}\gamma_\mu\ell], \\ O_{10A} &= [\bar{s}\gamma^\mu(1-\gamma_5)b][\bar{\ell}\gamma_\mu\gamma_5\ell]. \end{aligned} \tag{7}$$

For example, the diagram in Fig. 1 gives a contribution from O^w_{RL} (denoted by ⊗) to $O_{7\gamma}$. The coefficients of the QCD and electroweak penguin operators, $O_{3,\ldots,10}$, are also modified, but their effect on the processes we consider are suppressed.

Summing the relevant diagrams, the contributions of all operators can be expressed in terms of generalized Inami-Lim functions, presented in the Appendix. Setting $\Lambda = 1$ TeV, the numerical results are[2]

$$\begin{aligned} C_{7\gamma}(m_W) &= -0.193 + (0.810C^u_{LL} + 0.179C^h_{LL} + 0.310C^w_{RL} \\ &\quad - 0.236C^b_{RL} + 0.004C^w_{LR} - 0.003C^b_{LR}), \\ C_{9V}(m_W) &= \frac{\alpha}{2\pi}[1.56 + (-0.562C^u_{LL} + 44.95C^h_{LL} \\ &\quad - 0.885C^w_{RL} - 1.127C^b_{RL} + 0.046C^w_{LR} \\ &\quad + 0.004C^b_{LR})], \\ C_{10A}(m_W) &= \frac{\alpha}{2\pi}[-4.41 + (-7.157C^u_{LL} - 598C^h_{LL} \\ &\quad + 3.50C^w_{RL} - 0.004C^u_{RR})]. \end{aligned} \tag{8}$$

The first term in each expression is the SM contribution. Note that the O^h_{LL} contribution is large because it is at tree level, while O^b_{LR}, O^w_{LR}, and O^u_{RR} are tiny because they are suppressed by m_c/m_W and so the constraints on these will be weaker. In the case of $b \to d$ transitions the NP contribution has to be rescaled by the $\mathcal{O}(1/\lambda)$ factor, $|V^*_{ts}V_{ud}/V^*_{td}V_{cs}| \approx 5.6$, and C_i should be replaced with C'_i.

C. $\Delta F = 2$ transitions

The operators O^u_{LL}, C^h_{LL}, and O^w_{RL} also contribute to $\Delta F = 2$ transitions, i.e., neutral meson mixings. Again, the contribution from O^h_{LL} is present at tree level, while the

[2]Throughout this paper we will bound $C_i(1\ \text{TeV}/\Lambda)^2$ and quote numerical results setting $\Lambda = 1$ TeV.

other two contribute starting at one-loop order. The relevant functions are again listed in the Appendix. The modifications relative to the SM Inami-Lim function can be parametrized as $S_0 \to S_0(1 + h_M e^{2i\sigma_M})$ for each neutral meson system. Numerically (setting $\Lambda = 1$ TeV), for $B_s^0\bar{B}_s^0$ mixing, the effect of the $t \to c$ operators is given by

$$h_{B_s} e^{2i\sigma_{B_s}} = 800(C_{LL}^h)^2 + 0.92 C_{LL}^h C_{LL}^u - 6.84(C_{LL}^u)^2 + 1.55 C_{LL}^h - 2.64 C_{LL}^u - 0.32(C_{RL}^w)^2 - 1.03 C_{RL}^w. \quad (9)$$

The contribution of the O_i' operators to $B_s^0\bar{B}_s^0$ mixing is given by replacing C_i with C_i' in Eq. (9) and multiplying its right-hand side by λ.

The contribution of the O_i operators to $B_d^0\bar{B}_d^0$ mixing is obtained by multiplying the right-hand side of Eq. (9) by $e^{i\beta}$, where β is the CKM phase, $\beta = \arg(-V_{cd}V_{cb}^*/V_{td}V_{tb}^*)$, whereas the contribution of the O_i' operators to $B_d^0\bar{B}_d^0$ mixing is obtained again by replacing C_i with C_i' in Eq. (9) and multiplying its right-hand side by $-e^{i\beta}/\lambda$.

Finally, the O_i' contribution to $K^0\bar{K}^0$ mixing is the same as that to $B_d^0\bar{B}_d^0$ mixing, up to corrections suppressed by powers of λ. For the O_i contribution to $K^0\bar{K}^0$ mixing, one has to replace in Eq. (9) each Wilson coefficient C_i by $C_i + C_i^* e^{i\beta}$ [see Eq. (A20) in the Appendix], and add to it the additional contribution

$$\Delta(h_K e^{2i\sigma_K}) = 2.26\,\mathrm{Re}(C_{LL}^h C_{LL}^u)e^{i\beta} - 5.17|C_{LL}^u|^2 e^{i\beta} - 8.35|C_{RL}^w|^2 e^{i\beta}. \quad (10)$$

These expressions are valid up to corrections suppressed by λ^2 or more.

IV. EXPERIMENTAL CONSTRAINTS

In this section we use low energy measurements to constrain the Wilson coefficients of the operators in Eq. (2). Throughout we assume that there are no cancellations between the contributions from different operators.

A. Direct bounds

The best direct bounds on the operators in Eq. (2), as summarized in [9], come at present from searches for FCNCs at the Tevatron, CERN LEP, and Hadron Electron Ring Accelerator. The strongest direct constraints on $t \to cZ$ and $t \to uZ$ come from an OPAL search for $e^+e^- \to \bar{t}c$ in LEP II [13]. The upper limit on the branching ratio $\mathcal{B}(t \to cZ, uZ) < 0.137$ bounds the LL and RR operators. For neutral currents involving a photon there is a constraint from ZEUS, which looked for $e^\pm p \to e^\pm tX$ [14]. This bounds $\mathcal{B}(t \to u\gamma) < 0.0059$, and is the strongest constraint on the RL and LR operators with an up quark. The other bounds come from a CDF search in Tevatron run I, which bounds $\mathcal{B}(t \to c\gamma, u\gamma) < 0.032$ [15] and constrains the LR and RL involving a charm. We translate these branching ratios into bounds on the Wilson coefficients and list them in the first rows of Tables I and II. The LHC reach with 100 fb^{-1} data, as estimated in the ATLAS study [1], is $\mathcal{B}(t \to cZ, uZ) < 5.5 \times 10^{-5}$ and $\mathcal{B}(t \to c\gamma, u\gamma) < 1.2 \times 10^{-5}$. This will improve the current direct constraints on the Wilson coefficients by one-and-a-half orders of magnitude, as summarized in the second rows of the tables.

B. $B \to X_s\gamma$ and $B \to X_s\ell^+\ell^-$

We first consider the constraints from $B \to X_s\gamma$. At the scale m_b, $O_{7\gamma}$ gives the leading contribution. Using the next-to-leading order SM formulas from Ref. [16], we obtain

$$\mathcal{B}(B \to X_s\gamma) = 10^{-4} \times (0.07 + |1.807 + 0.081i + 1.81\Delta C_{7\gamma}(m_W)|^2), \quad (11)$$

where $\Delta C_{7\gamma}(m_W)$ is the NP contribution to $C_{7\gamma}$ at the $\mu = m_W$ matching scale. The current experimental average [17], $\mathcal{B}(B \to X_s\gamma) = (3.55 \pm 0.26) \times 10^{-4}$, implies at 95% CL[3] (setting $\Lambda = 1$ TeV)

$$\begin{aligned} -0.07 < C_{LL}^u < 0.04 \quad &\text{or} \quad 1.2 < C_{LL}^u < 1.3, \\ -0.3 < C_{LL}^h < 0.16 \quad &\text{or} \quad 5.3 < C_{LL}^h < 5.8, \\ -0.2 < C_{RL}^w < 0.1 \quad &\text{or} \quad 3.1 < C_{RL}^w < 3.4, \\ -0.1 < C_{RL}^b < 0.24 \quad &\text{or} \quad -4.5 < C_{RL}^b < -4.1. \end{aligned} \quad (12)$$

The first (left) intervals are consistent with the SM, while the second (right) ones require new physics at the $\mathcal{O}(1)$ level. The non-SM region away from zero is disfavored by $b \to s\ell^+\ell^-$ discussed below, but we include it here for completeness. For the operators whose contributions are suppressed by m_c, we find

$$-14 < C_{LR}^w < 7, \qquad -10 < C_{LR}^b < 19, \quad (13)$$

and no meaningful bound for C_{RR}^u. To obtain the results in Eqs. (12) and (13), we assumed that the NP contributions are real relative to the SM, i.e., that there are no new CP violating phases. Had we not made this assumption, the allowed regions would be annuli in the complex C_i planes.

Next we consider $B \to X_s\ell^+\ell^-$. The theoretically cleanest bound at present comes from the inclusive $B \to X_s\ell^+\ell^-$ rate measured for 1 GeV$^2 < q^2 < 6$ GeV^2 [18],

$$\mathcal{B}(B \to X_s\ell^+\ell^-)_{1\ \mathrm{GeV}^2 < q^2 < 6\ \mathrm{GeV}^2} = (1.61 \pm 0.51) \times 10^{-6}. \quad (14)$$

Because of the unusual power counting in $B \to X_s\ell^+\ell^-$, the full set of $\mathcal{O}(\alpha_s)$ corrections are only included in what is called next-to-next-to-leading logarithmic (NNLL) or-

[3]Hereafter all constraints are quoted at 95% CL, unless otherwise specified.

der, achieving an accuracy around 10%. For the SM prediction we use the NNLL calculation as implemented in Ref. [19]. This calculation does not normalize the rate to the $B \to X \ell \bar{\nu}$ rate; doing so would not improve the prediction significantly and would unnecessarily couple different operators' contributions. We include the modifications of $C_{7\gamma}$, C_{9V}, and C_{10A} due to the new operators at lowest order. With our input parameters, we obtain

$$\begin{aligned}\mathcal{B}(B \to X_s \ell^+ \ell^-)_{1<q^2<6\ \mathrm{GeV}^2} = 10^{-6} \times \{1.55 + 35\,100[|\Delta C_{9V}(m_W)|^2 + |\Delta C_{10A}(m_W)|^2] + 0.45|\Delta C_{7\gamma}(m_W)|^2 \\ + \mathrm{Re}[(180 + 5i)\Delta C_{9V}(m_W)] - 360\,\mathrm{Re}[\Delta C_{10A}(m_W)] - \mathrm{Re}[(0.17 + 0.04i)\Delta C_{7\gamma}(m_W)] \\ - 200\,\mathrm{Re}[\Delta C_{9V}(m_W)^* \Delta C_{7\gamma}(m_W)]\}. \end{aligned} \tag{15}$$

The simplest way to proceed would be to bound $C_{7\gamma}$, C_{9V}, and C_{10A} separately at $\mu = m_W$, assuming that the others have their SM values, and use this to constrain new physics. This procedure would not be consistent, since the NP necessarily affects these Wilson coefficients in a correlated way. Instead, we directly constrain the coefficients of O^u_{LL}, O^h_{LL}, O^w_{LR}, and O^b_{LR}, which also yields stronger constraints. With $\Lambda = 1$ TeV, we obtain

$$\begin{aligned} -1.1 < C^u_{LL} < 0.3, \\ -1.8 \times 10^{-2} < C^h_{LL} < -1 \times 10^{-2} \quad \text{or} \quad -5 \times 10^{-3} < C^h_{LL} < 3 \times 10^{-3}, \\ -0.5 < C^w_{RL} < 0.7 \quad \text{or} \quad 1.7 < C^w_{RL} < 3, \\ -2.0 < C^b_{RL} < 3.5. \end{aligned} \tag{16}$$

The combined constraints from $B \to X_s \gamma$ and $B \to X_s \ell^+ \ell^-$ on these four Wilson coefficients are shown in Table I in the Conclusions. We plot in Fig. 2 the bound on the LL operators in the $C^u_{LL} - C^h_{LL}$ plane. The SM corresponds to the point (0, 0). A measurement or a bound on the $t \to cZ$ branching ratio corresponds to a nearly vertical band. The LHC is sensitive to this whole plane, except for the band between the dashed lines.

The above bounds were derived assuming that the NP contribution is real relative to the SM. It is conceivable that improved measurements of $B \to X_s \ell^+ \ell^-$ will lead to constraints on the CP violating phases before the LHC is able to probe top FCNCs. Thus we postpone a full analysis with complex NP Wilson coefficients until more data become available.

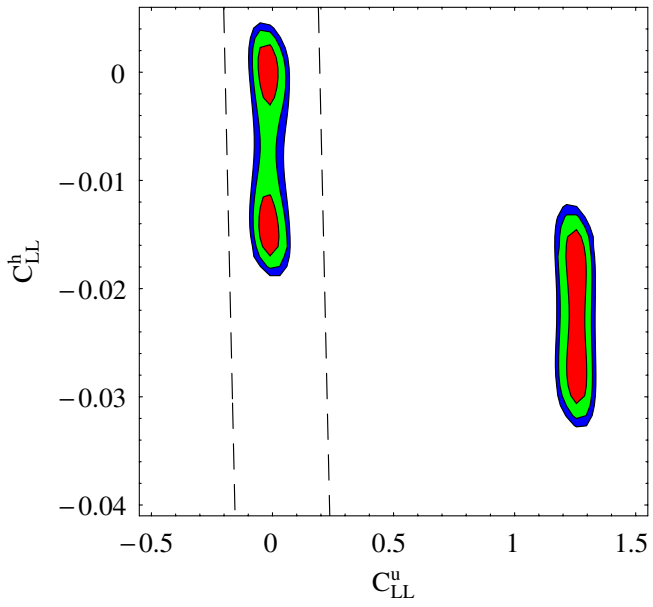

FIG. 2 (color online). Constraints from $B \to X_s \gamma$ and $B \to X_s \ell^+ \ell^-$ in the $C^u_{LL} - C^h_{LL}$ plane. The red (inner), green (middle), and blue (outer) regions denote 68%, 95%, and 99% CL, respectively. The region between the dashed lines is beyond the LHC sensitivity.

C. Exclusive and inclusive $b \to c \ell \bar{\nu}$ decays

In this subsection we investigate the constraints on the operators in Eq. (2) due to measurements of semileptonic $b \to c$ decays. They will allow us to bound the coefficient of the operator O^w_{LR}, which contains a right-handed charm field and is weakly constrained otherwise. We focus on three types of constraints coming from the ratio of exclusive D and D^* rates, the polarization in the D^* mode, and moments in inclusive spectra.

We begin with the exclusive case where the $B \to D \ell \nu$ and $B \to D^* \ell \nu$ rates can be calculated in an expansion in $\Lambda_{\mathrm{QCD}}/m_{b,c}$ using heavy quark effective theory. The form factors at zero recoil, where $w = v \cdot v' = 1$ (v and v' are the four-velocities of the B and $D^{(*)}$ mesons, respectively), have been determined from lattice QCD [20]. In the SM the ratio of rates is independent of V_{cb}, and therefore it provides a good test for non-SM contributions. The presence of the new operator, O^w_{LR}, affects the two rates differently. The rates are given by [21]

$$\begin{aligned} \frac{d\Gamma(B \to D \ell \nu)}{dw} &= \frac{G_F^2 m_B^5}{48\pi^3} r^3 (w^2 - 1)^{3/2} (1 + r)^2 |V_{cb}|^2 (\mathcal{F}_D)^2, \\ \frac{d\Gamma(B \to D^* \ell \nu)}{dw} &= \frac{G_F^2 m_B^5}{48\pi^3} r^{*3} \sqrt{w^2 - 1} (1 + w)^2 \\ &\quad \times \left[(1 - r^*)^2 + \frac{4w}{1 + w} (1 - 2wr^* + r^{*2}) \right] \\ &\quad \times |V_{cb}|^2 (\mathcal{F}_{D^*})^2, \end{aligned} \tag{17}$$

where $r = m_D/m_B$ and $r^* = m_{D^*}/m_B$. The form factors $\mathcal{F}_{\mathcal{D}}$ and $\mathcal{F}_{\mathcal{D}^*}$ can be decomposed in terms of 6 form factors, $h_{+,-,V,A_1,A_2,A_3}$ [21]. At leading order in the heavy quark limit, $\mathcal{F}(w) = \mathcal{F}^*(w) = h_{+,V,A_1,A_3} = \xi(w)$, where $\xi(w)$ is the Isgur-Wise function [22], while $h_{-,A_2} = 0$. Therefore, it is useful to define the following ratios of form factors:

$$R_1(w) = \frac{h_V}{h_{A_1}}, \qquad R_2(w) = \frac{h_{A_3} + r^* h_{A_2}}{h_{A_1}}, \tag{18}$$

which are equal to unity in the heavy quark limit and have been measured experimentally.

Following the analysis of [23], we can absorb the new physics contributions in the form factors. We obtain

$$\begin{aligned}
\Delta h_+ &= k(1+r)(1-w)\xi(w),\\
\Delta h_- &= -k(1-r)(1+w)\xi(w),\\
\Delta h_{A_1} &= -2k(1-r^*)\xi(w),\\
\Delta h_{A_2} &= -2k\xi(w),\\
\Delta h_{A_3} &= -2k\xi(w),\\
\Delta h_V &= 2k(1+r^*)\xi(w),
\end{aligned} \tag{19}$$

where

$$k = \frac{2vm_B}{\Lambda^2}\,\mathrm{Re}\left(\frac{C^w_{LR}V_{tb}}{V_{cb}}\right). \tag{20}$$

For the new physics contribution we include only the leading term, so we set $\xi(1) = 1$. Setting $\Lambda = 1$ TeV, we obtain

$$\begin{aligned}
\mathcal{F}_D(1) &\approx \mathcal{F}_D^{\mathrm{SM}}(1) - 1.01\times 10^{-3}\times \mathrm{Re}\left(\frac{C^w_{LR}V_{tb}}{V_{cb}}\right),\\
\mathcal{F}_{D^*}(1) &\approx \mathcal{F}_{D^*}^{\mathrm{SM}}(1) - 2.02\times 10^{-3}\times \mathrm{Re}\left(\frac{C^w_{LR}V_{tb}}{V_{cb}}\right),\\
R_1(1) &\approx R_1^{\mathrm{SM}}(1) + 6.52\times 10^{-3}\times \mathrm{Re}\left(\frac{C^w_{LR}V_{tb}}{V_{cb}}\right),\\
R_2(1) &\approx R_2^{\mathrm{SM}}(1) - 2.48\times 10^{-3}\times \mathrm{Re}\left(\frac{C^w_{LR}V_{tb}}{V_{cb}}\right).
\end{aligned} \tag{21}$$

Recent lattice QCD calculations [20] give $\mathcal{F}_D^{\mathrm{SM}}(1) = 1.074 \pm 0.024$ and $\mathcal{F}_{D^*}^{\mathrm{SM}}(1) = 0.91 \pm 0.04$. For R_1^{SM} and R_2^{SM} we use the results of [24], scanning over the hadronic parameters that enter. The experimental results are $|V_{cb}|\mathcal{F}_D(1) = (42.4 \pm 4.4)\times 10^{-3}$, $|V_{cb}|\mathcal{F}_{D^*}(1) = (36.2 \pm 0.6)\times 10^{-3}$ [17], $R_1(1) = (1.417 \pm 0.075)$, and $R_2(1) = (0.836 \pm 0.043)$ [25]. We set $|V_{tb}| = 1$ and do a combined fit for C^w_{LR} and $|V_{cb}|$. We find

$$-0.2 < \frac{\mathrm{Re}(V^*_{cb}C^w_{LR}V_{tb})}{|V_{cb}|} < 1.6. \tag{22}$$

We next turn to inclusive $B \to X_c\ell\bar\nu$ decays, which are also sensitive to the presence of the additional operators. We concentrate on the partial branching ratio and moments constructed from the charged lepton energy spectrum (see, e.g., [26]),

$$\begin{aligned}
M_0(E_0) &= \tau_B \int_{E_0} \frac{\mathrm{d}\Gamma}{\mathrm{d}E_\ell}\mathrm{d}E_\ell, \qquad M_1(E_0) = \frac{\int_{E_0} E_\ell \frac{\mathrm{d}\Gamma}{\mathrm{d}E_\ell}\mathrm{d}E_\ell}{\int_{E_0}\frac{\mathrm{d}\Gamma}{\mathrm{d}E_\ell}\mathrm{d}E_\ell},\\
M_k(E_0) &= \frac{\int_{E_0}[E_\ell - M_1(E_0)]^k \frac{\mathrm{d}\Gamma}{\mathrm{d}E_\ell}\mathrm{d}E_\ell}{\int_{E_0}\frac{\mathrm{d}\Gamma}{\mathrm{d}E_\ell}\mathrm{d}E_\ell}.
\end{aligned} \tag{23}$$

These are well measured and can be reliably calculated. We use the SM prediction including $1/m_b^2$ and α_s corrections and compare it in a combined fit with the 20 *BABAR* measurements [27] and a subset [28] of the 45 Belle [29] measurements, including their correlations. The modification of $\mathrm{d}\Gamma/\mathrm{d}E_\ell$ due to the C^w_{LR} coupling is given by

$$\begin{aligned}
\frac{\mathrm{d}\Gamma^{\mathrm{NP}}(B\to X_c\ell\bar\nu)}{\mathrm{d}y} &= -\frac{G_F^{5/2}m_b^6 v^2\,\mathrm{Re}(C^w_{LR}V_{cb})}{6\sqrt[4]{2}\pi^3\Lambda^2}\\
&\quad\times \frac{\sqrt{\rho}y^2(3-y)(1-y-\rho)^3}{(1-y)^3}\\
&\quad + \frac{\sqrt{2}G_F^3 m_b^7 v^4 |C^w_{LR}|^2}{3\pi^3\Lambda^4}\\
&\quad\times \frac{y^2(3-y)(1-y-\rho)^4}{(1-y)^3},
\end{aligned} \tag{24}$$

where $y = 2E_\ell/m_b$ and $\rho = m_c^2/m_b^2$. It is known that the data cannot be fitted well with the operator product expansion truncated at $1/m_b^2$. Including the $1/m_b^3$ corrections in a more complicated fit would make the agreement with the SM better, and therefore our bounds stronger.

The combined constraints on C^w_{LR} and $|V_{cb}|$ from exclusive and inclusive decays are shown in Fig. 3. The solid curves show the constraints from inclusive decays, the dashed curves show the bounds from exclusive semileptonic decays to D and D^*, and the shaded regions show the combined constraints (the confidence levels are as in Fig. 2).

D. Exclusive and inclusive $b \to u\ell\bar\nu$ decays

We now turn to some 3rd → 1st generation transitions. While the experimental constraints are less precise for these than for 3rd → 2nd generation transitions, the SM also predicts smaller rates, and therefore NP could more effectively compete with the SM processes. These constraints are particularly important as they bound the O_i' contributions relevant for $t \to u$ decays, which might not be distinguishable at the LHC from $t \to c$.

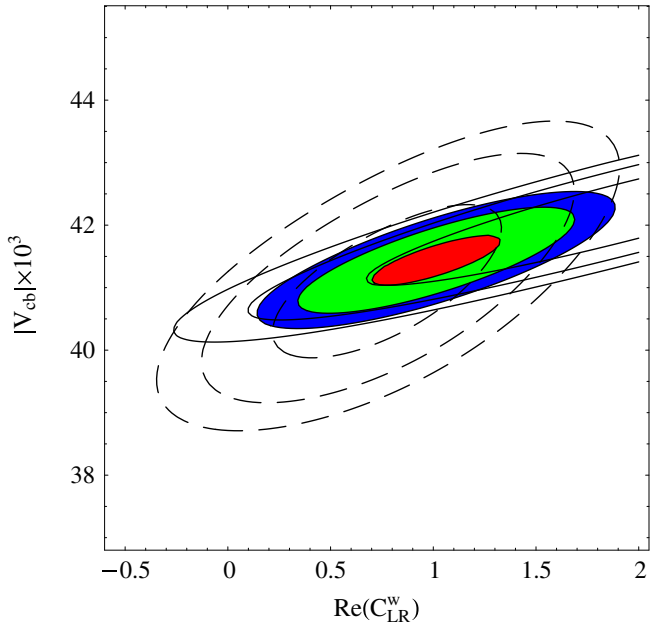

FIG. 3 (color online). Constraints on O^{w}_{LR} in the $\mathrm{Re}(C^{w}_{LR}) - |V_{cb}|$ plane from semileptonic $B \to X_c \ell \bar{\nu}$ (solid curves) and $B \to D^{(*)} \ell \bar{\nu}$ decays (dashed curves) and their combination (shaded areas). For each constraint the 68%, 95%, and 99% CL regions are shown.

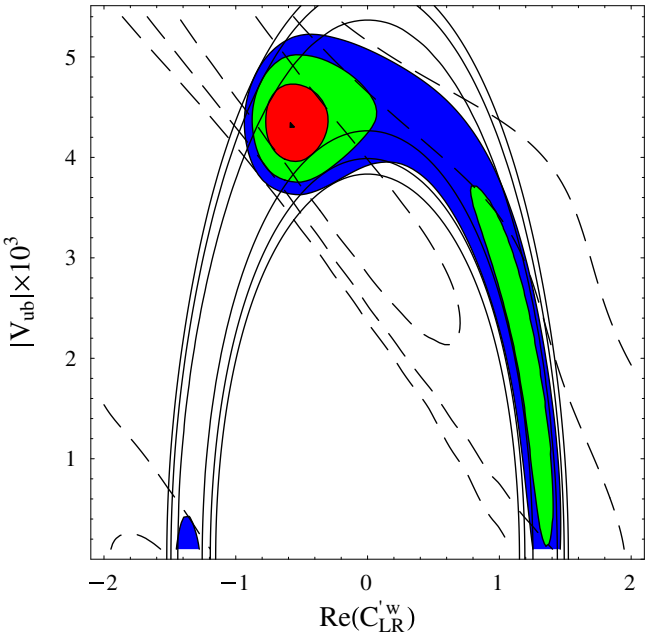

FIG. 4 (color online). Constraints on O'^{w}_{LR} in the $\mathrm{Re}(C'^{w}_{LR}) - |V_{ub}|$ plane from $B \to X_u \ell \bar{\nu}$ (solid curves) and $B \to \pi \ell \bar{\nu}$ (dashed curves) and their combination (shaded areas). For each constraint the 68%, 95%, and 99% CL regions are shown.

As is the case for 3rd → 2nd generation transitions, exclusive and inclusive semileptonic $b \to u$ decays can constrain the operator O'^{w}_{LR} in $t \to u$ transitions. Similarly to $b \to c \ell \bar{\nu}$, this operator distorts the lepton energy spectrum, so information on the lepton energy moments could constrain it. However, such measurements are not yet available for $B \to X_u \ell \bar{\nu}$. Therefore, to distinguish between the SM V_{ub} contribution and C^{w}_{LR}, we use $B \to \pi \ell \bar{\nu}$ in addition to the inclusive data.

For exclusive $B \to \pi \ell \bar{\nu}$ decay, we use for the SM prediction the parametrization of Ref. [30], which relies on analyticity constraints and lattice QCD calculations of the form factors at large q^2 [31,32]. The NP contribution is

$$\frac{d\Gamma^{\mathrm{NP}}(B \to \pi \ell \bar{\nu})}{dq^2} = \frac{G_F^2 |p_\pi|^3}{24\pi^3} \Big\{ \frac{4 m_B^2 v^2 |C'^{w}_{LR}|^2}{\Lambda^4} [(1+\hat{q}^2) f_- + (1-\hat{q}^2) f_+]^2 - \frac{4 m_B v \, \mathrm{Re}(V_{tb} C^{w}_{LR} V^*_{ub})}{\Lambda^2} \times [(1-\hat{q}^2) f_+^2 + (1+\hat{q}^2) f_- f_+] \Big\}, \quad (25)$$

where the $f_\pm$ form factors are functions of the dilepton invariant mass, q^2, $\hat{q}^2 = q^2/m_B^2$, and we neglected terms suppressed by m_π^2/m_B^2.

For inclusive $B \to X_u \ell \bar{\nu}$ decay, we focus on the measurement utilizing combined cuts [33] on q^2 and the hadronic invariant mass m_X, and compare it with the Belle and *BABAR* measurements [34]. Using this determination of V_{ub} is particularly simple for our purposes, because in the large q^2 region the mild cut on m_X used in the analysis only modifies the rate at a subleading level. Working to leading order in the NP contribution, we can neglect the effect of the m_X cut on the NP and include the NP contribution to the rate via

$$\frac{d\Gamma^{\mathrm{NP}}(B \to X_u \ell \bar{\nu})}{dq^2} = \frac{G_F^2 m_b^5}{192\pi^3} \frac{32 m_B^2 v^2}{\Lambda^4} |C'^{w}_{LR}|^2 \hat{q}^2 (\hat{q}^2 - 1)^2 \times (\hat{q}^2 + 2). \quad (26)$$

Since the interference between the SM and NP is suppressed by m_u/m_b [see the $\sqrt{\rho}$ factor in Eq. (24) in the first term], there is no dependence on the weak phase of C'^{w}_{LR} in the inclusive decay. Using other determinations of V_{ub} would be harder to implement and would not change our results significantly.

The combined constraint on C'^{w}_{LR} and $|V_{ub}|$ from inclusive and exclusive decays is shown in Fig. 4. (This uses the lattice QCD input from Fermilab [31], and the one using the HPQCD calculation [32] would also be similar.)

E. $B \to \rho\gamma$ and $B \to \mu^+\mu^-$

The inclusive $B \to X_d \gamma$ decay has not been measured yet, and there is only limited data on $B \to \rho\gamma$. Averaging

the measurements [35] using the isospin-inspired[4] relation $\mathcal{B}(B \to \rho\gamma) = \mathcal{B}(B^\pm \to \rho^\pm\gamma) = 2(\tau_{B^\pm}/\tau_{B^0})\mathcal{B}(B^0 \to \rho^0\gamma)$, and the PDG value $\tau_{B^\pm}/\tau_{B^0} = 1.07$, we obtain

$$\mathcal{B}(B \to \rho\gamma) = (1.26 \pm 0.23) \times 10^{-6}. \quad (27)$$

To reduce the sensitivity to form factor models, we normalize this rate to $\mathcal{B}(B \to K^*\gamma) = [\mathcal{B}(B^\pm \to K^{*\pm}\gamma) + (\tau_{B^\pm}/\tau_{B^0})\mathcal{B}(B^0 \to K^{*0}\gamma)]/2 = (41.4 \pm 1.7) \times 10^{-6}$,

$$\frac{\mathcal{B}(B \to \rho\gamma)}{\mathcal{B}(B \to K^*\gamma)} = \left|\frac{V_{td}}{V_{ts}}\right|^2 \left(\frac{m_B^2 - m_\rho^2}{m_B^2 - m_{K^*}^2}\right) \xi_\gamma^{-2} \frac{|C_{7\gamma}|^2}{|C_{7\gamma}^{\rm SM}|^2}. \quad (28)$$

We use $\xi_\gamma = 1.2 \pm 0.15$, where this error estimate accounts for the fact that we consider the rates to be determined by $O_{7\gamma}(m_b)$ alone. The contributions of other operators have larger hadronic uncertainties and are expected to partially cancel [36]. If first principles lattice QCD calculations of the form factor become available, then one can avoid taking the ratio in Eq. (28), and directly compare the calculation of $\mathcal{B}(B \to \rho\gamma)$ with data. We obtain the following constraints:

$$\begin{aligned} -0.26 < C'^{u}_{LL} < -0.21 \quad &\text{or} \quad -0.026 < C'^{u}_{LL} < 0.03, \\ -1.2 < C'^{h}_{LL} < -0.9 \quad &\text{or} \quad -0.11 < C'^{h}_{LL} < 0.13, \\ -0.7 < C'^{w}_{RL} < -0.5 \quad &\text{or} \quad -0.07 < C'^{w}_{RL} < 0.08, \\ -0.1 < C'^{b}_{RL} < 0.09 \quad &\text{or} \quad 0.7 < C'^{b}_{RL} < 0.9. \end{aligned} \quad (29)$$

Note that there are no constraints on O'^{w}_{LR} or O'^{b}_{LR}, because of their m_u/m_W suppression. As for $B \to X_s\gamma$, the two solutions in Eq. (29) correspond to the sign ambiguity in interpreting the constraint on $|C_{7\gamma}|^2$ when we assume that the NP contributions are real relative to the SM. Had we not made this assumption, the allowed regions would be annuli in the complex C'_i planes.

The NP operators we consider also contribute to the rare decays $B_{d,s} \to \mu^+\mu^-$. This is most interesting for $B_d \to \mu^+\mu^-$, since one expects that the NP contribution is enhanced compared to the SM by $[(v^2/\Lambda^2)(1/|V_{td}|)]^2$, which is around 20 for $\Lambda = 1$ TeV. Moreover, O'^{h}_{LL} contributes at tree level, so its contribution is enhanced by an additional factor of $(4\pi/\alpha)^2$. Although this decay mode has not yet been observed and the present upper bound $\mathcal{B}(B \to \mu^+\mu^-) < 3 \times 10^{-8}$ [37] is 2 orders of magnitude above the SM expectation, it still gives a useful constraint on O'^{h}_{LL}. In particular, for $\Lambda = 1$ TeV, we obtain

$$-0.023 < C'^{h}_{LL} < 0.026. \quad (30)$$

[4]Isospin is not a symmetry of the electromagnetic interaction. This average relies on the heavy quark limit to argue that the dominant isospin violation is $\Lambda_{\rm QCD}/m_b$ suppressed. With more precise data, using only B^0 decays will be theoretically cleaner, because annihilation is suppressed in the B^0 compared to the $B^\pm$ modes. At present, this would double the experimental error, so we include the $B^\pm$ data.

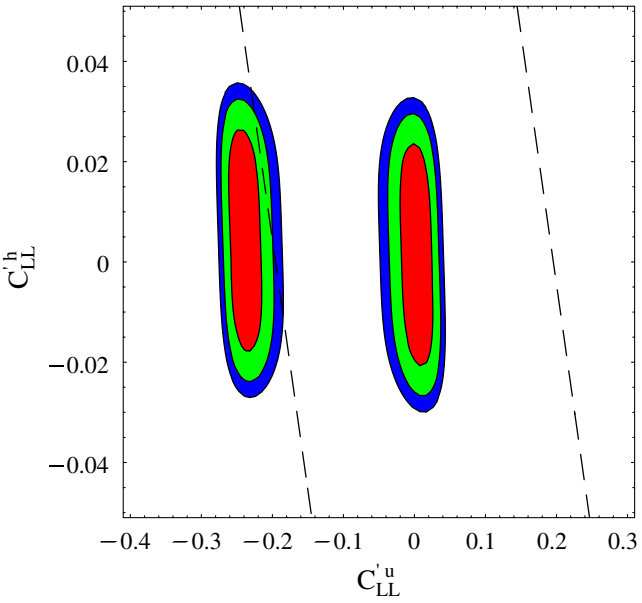

FIG. 5 (color online). Constraints from $B \to \rho\gamma$ and $B \to \mu^+\mu^-$ in the $C'^{u}_{LL} - C'^{h}_{LL}$ plane. The red (inner), green (middle), and blue (outer) regions denote 68%, 95%, and 99% CL, respectively. The region between the dashed lines is beyond the LHC sensitivity.

The combined constraints from $B \to \rho\gamma$ and $B \to \mu^+\mu^-$ on O'^{u}_{LL} and O'^{h}_{LL} are shown in Fig. 5. The region between the dashed lines is beyond the LHC reach, but the LHC will be able to exclude (though perhaps not completely) the non-SM region in Fig. 5. In the case of O'^{u}_{LL} and O'^{w}_{RL} the present data are not strong enough to exclude the non-SM region allowed by $B \to \rho\gamma$.

F. $\Delta F = 2$ transitions

In this section we present the results of the analysis of the NP effects in $\Delta F = 2$ processes. Since their contribution appear at the same time in $B_d\bar{B}_d$, $B_s\bar{B}_s$, and $K^0\bar{K}^0$, we performed a full fit using the CKMFITTER code [10], after having suitably modified it to include the results of Sec. III C. The code simultaneously fits experimental data for the Wolfenstein parameters $\bar{\rho}$ and $\bar{\eta}$ and for NP (extending earlier studies in $\Delta F = 2$ processes [38,39]). The observables used here include the B_d and B_s mass differences, the time dependent CP asymmetries in $B \to J/\psi K$, the CP asymmetries in $B \to \pi\pi$, $\rho\rho$, $\rho\pi$, the ratio of $|V_{ub}|$ and $|V_{cb}|$ measured in semileptonic B decays, the CP asymmetries in $B \to DK$, the width difference in the $B_s\bar{B}_s$ system, $\Delta\Gamma_s$, the semileptonic CP asymmetry in B decays, $A_{\rm SL}$, and the indirect CP violation in K decays, ϵ_K. We allowed the NP Wilson coefficients to be complex and performed a scan over their phases. Thus, the results in this section are quoted in terms of the absolute values of the C_i and C'_i. Keeping only one operator at a time, we get

$$|C^u_{LL}| < 0.07, \quad |C^h_{LL}| < 0.014, \quad |C^w_{RL}| < 0.14,$$
$$|C'^u_{LL}| < 0.11, \quad |C'^h_{LL}| < 0.018, \quad |C'^w_{RL}| < 0.26. \tag{31}$$

As before, we also performed a combined analysis for the LL operators. This is particularly interesting for O'^u_{LL} and O'^h_{LL}, since until $B \to X_d \ell^+ \ell^-$ data become available, only $\Delta F = 2$ processes are sensitive to the complex phases. In general, allowing for a variation of the phases of C'^u_{LL} and C'^h_{LL}, a cancellation can occur between the two contributions and the above bounds are relaxed. If their absolute values satisfy $|C'^h_{LL}| \sim 0.1|C'^u_{LL}|$, then arbitrarily large values of the Wilson coefficients are allowed for some values of the phases. This possibility is ruled out when the $B \to \rho\gamma$ and $B \to \mu^+\mu^-$ constraints are included. Indeed, combining $\Delta F = 2$ with these measurements, we obtain

$$|C'^u_{LL}| < 0.26, \qquad |C'^h_{LL}| < 0.026. \tag{32}$$

V. COMBINED CONSTRAINTS AND CONCLUSION

In this paper, we studied constraints on flavor-changing neutral current top quark decays, $t \to cZ$, uZ, $c\gamma$, $u\gamma$. We used an effective field theory in which beyond the SM physics is integrated out. In the theory with unbroken electroweak symmetry the leading contributions to such FCNC top decays come from seven dimension-6 operators of Eq. (2). We assumed that the new physics scale Λ is sufficiently above the electroweak scale v to expand in v/Λ and neglect higher dimension operators. We find different and sometimes stronger constraints than starting with an effective theory which ignores $SU(2)_L$ invariance.

The 95% CL constraints on the Wilson coefficients of the operators involving 3rd and 2nd generation fields are summarized in Table I. We consider one operator at a time; i.e. we consider the case where there are no cancellations. The top two rows show the present direct constraints and the expected LHC bounds. The next three rows show the bounds from B physics. In the $B \to X_s\gamma$, $X_s\ell^+\ell^-$ row, the combined bounds from these processes are shown. The two allowed regions are obtained, neglecting the complex phases of the operators (see Fig. 2 and the discussion in Sec. IV B). This assumption can be relaxed in the future with more detailed data on $B \to X_s\ell^+\ell^-$. In the $\Delta F = 2$ row the numbers refer to upper bounds on the magnitudes of the Wilson coefficients and are derived allowing the phase to vary. The best bound for each operator is listed and then translated to a lower bound on the scale Λ (in TeV, assuming that the C's are unity), and to the maximal $t \to cZ$ and $t \to c\gamma$ branching ratios still allowed by each operator. The last row indicates whether a positive LHC signal could be explained by each of the operators alone. In this row, the star in "Closed*" for C^u_{LL} and C^h_{LL} refers to the fact that small values of these Wilson coefficients cannot give an observable top FCNC signal; however, there is an allowed region with cancellations between the SM and the NP, which may still give a signal. In the same row "Ajar" means that C^w_{RL} and C^b_{RL} cannot yield a LHC signal in $t \to cZ$ but may manifest themselves in $t \to c\gamma$. It is remarkable that the coefficients of several operators are better constrained by B physics than by FCNC top decays at the LHC.

Table II shows the constraints on the operators involving the 3rd and 1st generation quarks. We studied this because the LHC may not be able to distinguish between $t \to c$ and $t \to u$ FCNC decays, and these processes are also interesting in their own rights. In this case there are two allowed regions of C'^w_{LR} from semileptonic decays, as can be seen in Fig. 4. The entries in the "Combined bound" row show the result of the fit to all the B decay data above it, as discussed in Sec. IV F. We see from the last row that the LHC window remains open for all of the RR, LR, and RL operators, except O'^w_{RL}.

We conclude from Tables I and II that if the LHC sees FCNC t decays, then they must have come from LR or RR operators, unless there are cancellations. Moreover, if $t \to cZ$ is seen but $t \to c\gamma$ is not, then only O^u_{RR} could account for the data.

Our analysis used the currently available data and compared them to an estimate of the LHC reach with 100 fb^{-1}. However, by that time many of the constraints discussed above will improve, and new measurements will become available. The direct bounds will be improved by measurements from run II of the Tevatron in the near future. All the B decay data considered in this paper will improve, and the calculations for many of them may become more precise. Important ones (in no particular order) are as follows: (i) improved measurements of $B \to X_s\ell^+\ell^-$ to better constrain the magnitudes and especially the phases of C^u_{LL}, C^h_{LL}, C^w_{RL}, and C^b_{RL}; (ii) measurements of the lepton energy and the hadronic mass moments in $B \to X_u\ell\bar{\nu}$ to constrain C'^w_{LR}; (iii) improvements in $B \to \rho\gamma$ and measurements of $B \to X_d\gamma$ to reduce the uncertainties of C'^u_{LL}, C'^h_{LL}, C'^w_{RL}, and C'^b_{RL}; (iv) measurement of $B \to X_d\ell^+\ell^-$ to reduce the errors and constrain the weak phases of these last four coefficients. Additional information will also come from LHCb. For example, the measurement of the CP violating parameter $S_{B_s \to \psi\phi}$, the direct measurements of the CKM angle γ, and some of the above rare decays will help improve the constraints. With several of these measurements available, one can try to relax the no-cancellation assumption employed throughout our analysis. Note that not all NP-sensitive B factory measurements can be connected to FCNC top decays; e.g., the CP asymmetry $S_{K^*\gamma}$ is sensitive to right-handed currents in the down sector and cannot receive a sizable enhancement from the operators in Eq. (2). Thus, there are many ways in which there can be interesting interplay between measurements of or bounds on FCNC t and b quark decays.

TABLE I. The 95% CL constraints on the Wilson coefficients of the operators involving 3rd and 2nd generation fields for $\Lambda = 1$ TeV, and $\cdots$ denotes that there is no bound in that entry. The top two rows show the present direct constraints and the expected LHC bounds. The second part shows the bounds from B physics, which is then translated to a lower bound on the NP scale, Λ, and to the maximal $t \to cZ$ and $t \to c\gamma$ branching ratios each operator could still give rise to (the ATLAS sensitivities with 100 fb^{-1} are 5.5×10^{-5} and 1.2×10^{-5}, respectively). The last line concludes whether a positive LHC signal could be explained by each of the operators.

	C^u_{LL}	C^h_{LL}	C^w_{RL}	C^b_{RL}	C^w_{LR}	C^b_{LR}	C^u_{RR}
Direct bound	9.0	9.0	6.3	6.3	6.3	6.3	9.0
LHC sensitivity	0.20	0.20	0.15	0.15	0.15	0.15	0.20
$B \to X_s\gamma$, $X_s\ell^+\ell^-$	$[-0.07, 0.036]$	$[-0.017, -0.01]$ $[-0.005, 0.003]$	$[-0.09, 0.18]$	$[-0.12, 0.24]$	$[-14, 7]$	$[-10, 19]$	$\cdots$
$\Delta F = 2$	0.07	0.014	0.14	$\cdots$	$\cdots$	$\cdots$	$\cdots$
Semileptonic	$\cdots$	$\cdots$	$\cdots$	$\cdots$	[0.3, 1.7]	$\cdots$	$\cdots$
Best bound	0.07	0.014	0.15	0.24	1.7	6.3	9.0
Λ for $C_i = 1$ (min)	3.9 TeV	8.3 TeV	2.6 TeV	2.0 TeV	0.8 TeV	0.4 TeV	0.3 TeV
$\mathcal{B}(t \to cZ)$ (max)	7.1×10^{-6}	3.5×10^{-7}	3.4×10^{-5}	8.4×10^{-6}	4.5×10^{-3}	5.6×10^{-3}	0.14
$\mathcal{B}(t \to c\gamma)$ (max)	$\cdots$	$\cdots$	1.8×10^{-5}	4.8×10^{-5}	2.3×10^{-3}	3.2×10^{-2}	$\cdots$
LHC window	Closed*	Closed*	Ajar	Ajar	Open	Open	Open

TABLE II. Constraints on the Wilson coefficients of the operators involving 3rd and 1st generation fields. The entries in the table are analogous to Table I.

	C'^u_{LL}	C'^h_{LL}	C'^w_{RL}	C'^b_{RL}	C'^w_{LR}	C'^b_{LR}	C'^u_{RR}
Direct bound	9.0	9.0	2.7	2.7	2.7	2.7	9.0
LHC sensitivity	0.20	0.20	0.15	0.15	0.15	0.15	0.20
$B \to \rho\gamma$, $\mu^+\mu^-$	$[-0.26, -0.21]$ $[-0.026, 0.03]$	$[-0.023, 0.026]$	$[-0.7, -0.5]$ $[-0.07, 0.08]$	$[-0.1, 0.09]$ $[0.7, 0.9]$	$\cdots$	$\cdots$	$\cdots$
$\Delta F = 2$	0.11	0.02	0.26	$\cdots$	$\cdots$	$\cdots$	$\cdots$
Semileptonic	$\cdots$	$\cdots$	$\cdots$	$\cdots$	$[-0.9, 0.1]$ $[0.8, 1.4]$	$\cdots$	$\cdots$
Combined bound	0.10	0.02	0.16	0.9	1.4	2.7	9.0
Λ for $C_i = 1$ (min)	3.2 TeV	7.2 TeV	2.5 TeV	1.1 TeV	0.8 TeV	0.6 TeV	0.3 TeV
$\mathcal{B}(t \to uZ)$ (max)	1.6×10^{-5}	6.4×10^{-7}	4.1×10^{-5}	1.2×10^{-4}	3.2×10^{-3}	1.0×10^{-3}	0.14
$\mathcal{B}(t \to u\gamma)$ (max)	$\cdots$	$\cdots$	2.1×10^{-5}	6.7×10^{-4}	1.6×10^{-3}	5.9×10^{-3}	$\cdots$
LHC window	Closed	Closed	Ajar	Open	Open	Open	Open

If a FCNC top decay signal is observed at the LHC, the next question will be how to learn more about the underlying physics responsible for it. With a few tens of events one can start to do an angular analysis or study an integrated polarization asymmetry [40]. These could discriminate left-handed or right-handed operators (say, O^u_{RR} or O^u_{LL}). Such interactions could arise in models in which the top sector has a large coupling to a new physics sector, predominantly through right-handed couplings [41]. However, a full angular analysis that could also distinguish O^u_{RR} from O^w_{LR} requires large statistics, which is probably beyond the reach of the LHC.

The observation of FCNC top decays at the LHC would be a clear discovery of new physics, and therefore it would be extremely exciting. Our analysis shows that a LHC signal requires Λ to be less than a few TeV. This generically implies the presence of new particles with significant coupling to the top sector. If the new particles are colored, we expect that they will be discovered at the LHC. It would be gratifying to decipher the underlying structure of new physics from simultaneous information from top and bottom quark decays and direct observations of new heavy particles at the LHC.

ACKNOWLEDGMENTS

We acknowledge helpful discussions with Chris Arnesen and Iain Stewart on $B \to \pi\ell\bar{\nu}$ [30], Frank Tackmann on $B \to X_s\ell^+\ell^-$ [19], and Phillip Urquijo about the Belle measurement of $B \to X_c\ell\bar{\nu}$ [29]. P. F., M. P., and G. P. thank the Aspen Center for Physics for hospitality while part of this work was completed. The work of P. F., Z. L., and M. P. was supported in part by the Director, Office of Science, Office of High Energy Physics of the U.S. Department of Energy under Contract No. DE-AC02-05CH11231. M. S. was supported in part by the National Science Foundation under Grant No. NSF-PHY-0401513.

APPENDIX A: ANALYTIC EXPRESSIONS

We give the form of the operators of Eq. (2) after electroweak symmetry breaking, keeping only trilinear vertices which do not involve the Higgs:

$$O^u_{LL} = \frac{\sqrt{2}m_W^2}{g_2}(\bar{t}_L \not{W}^- s_L + \bar{b}_L \not{W}^+ c_L) + \frac{2m_Z m_W}{g_2}\bar{t}_L \not{Z} c_L + \ldots, \qquad O^h_{LL} = \frac{2m_Z m_W}{g_2}(\bar{t}_L \not{Z} c_L + \bar{b}_L \not{Z} s_L) + \ldots,$$

$$O^w_{RL} = m_W \bar{s}_L \sigma^{\mu\nu} t_R W^-_{\mu\nu} + \sqrt{2} m_W \bar{c}_L \sigma^{\mu\nu} t_R (c_w Z_{\mu\nu} + s_w A_{\mu\nu}) + \ldots, \qquad O^b_{RL} = \sqrt{2} m_W \bar{c}_L \sigma^{\mu\nu} t_R \left(s_w A_{\mu\nu} - \frac{s_w^2}{c_w} Z_{\mu\nu}\right) + \ldots,$$

$$O^w_{LR} = m_W \bar{b}_L \sigma^{\mu\nu} c_R W^-_{\mu\nu} + \sqrt{2} m_W \bar{t}_L \sigma^{\mu\nu} c_R (c_w Z_{\mu\nu} + s_w A_{\mu\nu}) + \ldots, \qquad O^b_{LR} = \sqrt{2} m_W \bar{t}_L \sigma^{\mu\nu} c_R \left(s_w A_{\mu\nu} - \frac{s_w^2}{c_w} Z_{\mu\nu}\right) + \ldots,$$

$$O^u_{RR} = \frac{2m_Z m_W}{g_2}\bar{t}_R \not{Z} c_R + \ldots. \tag{A1}$$

Here $s_w = \sin\theta_w$, $c_w = \cos\theta_w$, and the dots denote the Hermitian conjugate and the neglected vertices involving Higgs and higher numbers of fields. Throughout this paper the covariant derivative is defined as $D_\mu = \partial_\mu + igA^a_\mu \tau^a + ig' B_\mu$.

The analytic expressions for the contributions of the operators in Eq. (2) to the top FCNC partial widths are

$$\begin{aligned}\Gamma(t \to cZ) = \frac{m_t}{16\pi}\frac{v^2 m_t^2}{\Lambda^4}(1-y)^2\{&[|C^h_{LL} + C^u_{LL}|^2 + |C^u_{RR}|^2](1+2y) + 2g_2^2 \cos^2\theta_W (2+y) \\ &\times [|C^b_{LR}\tan^2\theta_W - C^w_{LR}|^2 + |C^b_{RL}\tan^2\theta_W - C^w_{RL}|^2] - 6\sqrt{2} g_2 \sin\theta_W \tan\theta_W \sqrt{y}\,\mathrm{Re}[(C^b_{RL})^*(C^h_{LL} + C^u_{LL}) \\ &- (C^b_{LR})^* C^u_{RR}] + 6\sqrt{2} g_2 \cos\theta_W \sqrt{y}\,\mathrm{Re}[(C^w_{RL})^*(C^h_{LL} + C^u_{LL}) - (C^w_{LR})^* C^u_{RR}]\},\end{aligned} \tag{A2}$$

$$\Gamma(t \to c\gamma) = \alpha m_t \frac{v^2 m_t^2}{\Lambda^4}(|C^b_{LR} + C^w_{LR}|^2 + |C^b_{RL} + C^w_{RL}|^2), \tag{A3}$$

where $y = m_Z^2/m_t^2$. The analogous expressions for $t \to u$ decays are obtained by replacing C_i by C'_i above. This expression makes it straightforward to relate the Wilson coefficients used in this paper with different notation present in the literature, which defines the couplings in the effective Lagrangian after electroweak symmetry breaking.

Next we present the analytic expression for the Wilson coefficients originating from the operators in Eq. (2). We use the $\overline{\mathrm{MS}}$ scheme and match at the scale $\mu = m_W$. It is easiest to express the results as modifying the Inami-Lim functions B_0, C_0, and D_0/D'_0, coming from box diagrams, Z penguins, and γ penguins, respectively. Using the standard normalization of the effective Hamiltonian,

$$\mathcal{H}_{\mathrm{eff}} = -\frac{G_F}{\sqrt{2}} V_{tb} V^*_{ts} \sum C_i O_i, \tag{A4}$$

the Wilson coefficients at the matching scale can be written as

$$\begin{aligned} C_{7\gamma} &= -\frac{1}{2} D'_0(x), \\ C_{9V} &= \frac{\alpha}{2\pi}\left[-\frac{1}{\sin^2\theta_W} B_0(x) + \left(\frac{1}{\sin^2\theta_W} - 4\right) C_0(x) - D_0(x)\right], \\ C_{10A} &= \frac{\alpha}{2\pi}\frac{1}{\sin^2\theta_W}[B_0(x) - C_0(x)], \end{aligned} \tag{A5}$$

where $x = m_t^2/m_W^2$. In the SM, we have the well-known expressions [12]

$$\begin{aligned} B_0(x) &= \frac{1}{4}\left[-\frac{x}{x-1} + \frac{x}{(x-1)^2}\ln x\right], \\ C_0(x) &= \frac{x}{8}\left[\frac{x-6}{x-1} + \frac{3x+2}{(x-1)^2}\ln x\right], \\ D_0(x) &= -\frac{4}{9}\ln x - \frac{19x^3 - 25x^2}{36(x-1)^3} + \frac{x^2(5x^2 - 2x - 6)}{18(x-1)^4}\ln x, \\ D'_0(x) &= \frac{8x^3 + 5x^2 - 7x}{12(x-1)^3} - \frac{3x^3 - 2x^2}{2(x-1)^4}\ln x. \end{aligned} \tag{A6}$$

The contributions of the O^u_{LL}, O^w_{LR}, and O^b_{LR} operators introduced in Eq. (2) can be included by adding the following terms to Eq. (A6):

$$\Delta B_0(x) = \frac{\kappa}{2} C^u_{LL}\left(\frac{1}{x-1} - \frac{x\ln x}{(x-1)^2}\right), \tag{A7}$$

$$\begin{aligned}\Delta C_0 = \frac{\kappa}{24} C^u_{LL}\Bigg(&\frac{20(x-1)\sin^2\theta_W + 23x + 7}{x-1} \\ &- \frac{6x(x^2 + x + 3)}{(x-1)^2}\ln x\Bigg) - \frac{2\pi\kappa}{\alpha_2} C^h_{LL} \\ &+ \frac{3\kappa g}{2\sqrt{2}} C^w_{RL}\sqrt{x}\left(\frac{x}{x-1} - \frac{x\ln x}{(x-1)^2}\right) \\ &- \frac{\kappa\sqrt{x x_c}}{8} C^u_{RR}\left(\frac{1}{2} - \frac{x-4}{x-1}\ln x\right),\end{aligned} \tag{A8}$$

$$\Delta D_0 = -\frac{\kappa}{9} C_{LL}^u \left(\frac{47x^3 - 237x^2 + 312x - 104}{6(x-1)^3} - \frac{3x^4 - 30x^3 + 54x^2 - 32x + 8}{(x-1)^4} \ln x \right) + \frac{\sqrt{2}\kappa g}{3} C_{RL}^w \sqrt{x} \left(\frac{49x^2 - 89x + 34}{6(x-1)^3} - \frac{6x^3 - 9x^2 + x + 1}{(x-1)^4} \ln x \right) - \sqrt{2}\kappa g C_{RL}^b \frac{\sqrt{x}\ln x}{x-1} + \frac{\kappa g \sqrt{x_c}}{\sqrt{2}} C_{LR}^w \left(\frac{59x - 68}{9(x-1)} + \frac{3x-2}{(x-1)^2} \ln x \right) + \frac{\kappa g \sqrt{x_c}}{\sqrt{2}} C_{LR}^b \frac{x-2}{x-1}, \tag{A9}$$

$$\Delta D_0' = \frac{\kappa}{2} C_{LL}^u \left(\frac{68x^3 - 291x^2 + 297x - 92}{18(x-1)^3} + \frac{x^2(3x-2)}{(x-1)^4} \ln x \right) + \frac{4\kappa}{27} C_{LL}^h (\sin^2\theta_W + 3) - \frac{\kappa g}{3\sqrt{2}} C_{RL}^w \sqrt{x} \left(\frac{3x^3 + 33x^2 - 25x + 1}{2(x-1)^3} - \frac{3x^4 - 6x^3 + 33x^2 - 32x + 8}{(x-1)^4} \ln x \right) + \frac{\kappa g}{2\sqrt{2}} C_{RL}^b \sqrt{x} \left(\frac{x-7}{x-1} - \frac{2x(x-4)}{(x-1)^2} \ln x \right) + \frac{2\sqrt{2}\kappa g \sqrt{x_c}}{3} C_{LR}^w - \frac{\kappa g \sqrt{x_c}}{\sqrt{2}} C_{LR}^b, \tag{A10}$$

where $x_c = m_c^2/m_W^2$ and

$$\kappa = \frac{v^2}{\Lambda^2} \frac{V_{cs}^*}{V_{ts}^*}. \tag{A11}$$

Note that the contribution of O_{LL}^h to ΔC_0 occurs at tree level, as indicated by its $1/\alpha_2$ enhancement in Eq. (A8), so O_{LL}^h gives tree-level contributions to C_{9V} and C_{10A}. Nevertheless, we shall not include the matrix element of O_{LL}^h to one higher order in α_2, in analogy with the conventional approach in which the NNLL calculation of $B \to X_s \ell^+ \ell^-$ does not include the $\mathcal{O}(\alpha_s^2)$ matrix element of O_{9V}.

Finally, we calculate the $\Delta F = 2$ contributions due to C_{LL}^u and C_{LR}^w. The shift in the SM contributions reads

$$S_0^{\rm SM} \to S_0^{\rm SM} + \kappa_i \Delta S_i(x) + \kappa_i \kappa_j \Delta S'_{i,j}(x) + \kappa_{ij} \Delta S''_{ij}(x), \tag{A12}$$

where $i = u, h, w$ labels the contributions from the operators O_{LL}^u, O_{LL}^h, and O_{RL}^w, respectively. The expressions for ΔS and $\Delta S'$ are

$$\Delta S_u = -\frac{x(4x^2 - 11x + 1)}{(x-1)^2} + \frac{2x(x^3 - 6x + 2)}{(x-1)^3} \ln x, \tag{A13}$$

$$\Delta S_h = -\frac{x[(1+x)\sin^2\theta_W + 2x - 6]}{x-1} + \frac{2x[x(x+2)\sin^2\theta_W - 6]}{3(x-1)^2} \ln x, \tag{A14}$$

$$\Delta S_w = 3g\sqrt{2x} \left[\frac{x(x+1)}{(x-1)^2} - \frac{2x^2}{(x-1)^3} \ln x \right], \tag{A15}$$

$$\Delta S'_{u,u} = \frac{7x^3 - 15x^2 + 6x - 4}{(x-1)^2} - \frac{2x(2x^3 + 3x^2 - 12x + 4)}{(x-1)^3} \ln x, \tag{A16}$$

$$\Delta S'_{h,h} = \frac{16\pi}{\alpha_2}, \tag{A17}$$

$$\Delta S'_{u,h} = \frac{2[(x+1)(x+2)\sin^2\theta_W + 3(x^2 - 9x + 4)]}{3(x-1)} + \frac{2x[x(x - 3 - 2\sin^2\theta_W) + 6]}{(x-1)^2} \ln x, \tag{A18}$$

$$\Delta S'_{w,w} = g^2 \left[-\frac{6x(x+1)}{(x-1)^2} + \frac{12x^2}{(x-1)^3} \ln x \right], \tag{A19}$$

and κ_i depends on the flavor transition,

$$\kappa_i = \frac{v^2}{\Lambda^2} \begin{cases} C_i V_{cs}/V_{ts} & \text{for } t \to c \text{ contribution in } b \to s \\ C_i V_{cd}/V_{td} & \text{for } t \to c \text{ contribution in } b \to d \\ C_i' V_{us}/V_{ts} & \text{for } t \to u \text{ contribution in } b \to s \\ C_i' V_{ud}/V_{td} & \text{for } t \to u \text{ contribution in } b \to d \\ (C_i V_{ts}^* V_{cd} + C_i^* V_{cs}^* V_{td})/(V_{ts}^* V_{td}) & \text{for } t \to c \text{ contribution in } s \to d \\ (C_i' V_{ts}^* V_{ud} + C_i'^* V_{us}^* V_{td})/(V_{ts}^* V_{td}) & \text{for } t \to u \text{ contribution in } s \to d. \end{cases} \tag{A20}$$

The κ_{ij} are zero except for $K^0\bar{K}^0$ mixing, where they are given by

$$\kappa_{ij} = \frac{v^4}{\Lambda^4}\begin{cases} C_i C_j^* V_{cs}^* V_{cd}/(V_{ts}^* V_{td}) & \text{for } t \to c \\ C_i' C_j'^* V_{us}^* V_{ud}/(V_{ts}^* V_{td}) & \text{for } t \to u, \end{cases} \tag{A21}$$

and $\Delta S_{ij}''$ are given by

$$\Delta S_{u,u}'' = \frac{x(29x^2 - 84x + 7)}{4(x-1)^2} - \frac{x(7x^3 + 9x^2 - 64x + 24)}{2(x-1)^3} \times \ln x, \tag{A22}$$

$$\Delta S_{u,h}'' = \frac{2x[2x - 6 + (x+1)\sin^2\theta_W]}{(x-1)} - \frac{4x[x(x+2)\sin^2\theta_W - 6]}{3(x-1)^2}\ln x, \tag{A23}$$

$$\Delta S_{w,w}'' = g^2\Big[-\frac{2x(x^2 - 2x - 11)}{(x-1)^2} - \frac{12x^2(x^2 - 3x + 4)}{(x-1)^3}\ln x\Big]. \tag{A24}$$

[1] J. Carvalho *et al.* (ATLAS Collaboration), Eur. Phys. J. C **52**, 999 (2007).

[2] G. L. Bayatian *et al.* (CMS Collaboration), J. Phys. G **34**, 995 (2007).

[3] F. Larios, R. Martinez, and M. A. Perez, Int. J. Mod. Phys. A **21**, 3473 (2006); J. L. Diaz-Cruz, R. Martinez, M. A. Perez, and A. Rosado, Phys. Rev. D **41**, 891 (1990); G. Eilam, J. L. Hewett, and A. Soni, Phys. Rev. D **44**, 1473 (1991) **59**, 039901(E) (1999); J. A. Aguilar-Saavedra and B. M. Nobre, Phys. Lett. B **553**, 251 (2003); J. A. Aguilar-Saavedra and G. C. Branco, Phys. Lett. B **495**, 347 (2000); J. A. Aguilar-Saavedra, Phys. Rev. D **67**, 035003 (2003); **69**, 099901(E) (2004); J. L. Diaz-Cruz and G. Lopez Castro, Phys. Lett. B **301**, 405 (1993); M. E. Luke and M. J. Savage, Phys. Lett. B **307**, 387 (1993); P. J. Fox *et al.*, arXiv:hep-th/0503249; B. Grzadkowski, J. F. Gunion, and P. Krawczyk, Phys. Lett. B **268**, 106 (1991); C. S. Li, R. J. Oakes, and J. M. Yang, Phys. Rev. D **49**, 293 (1994); **56**, 3156(E) (1997); G. M. de Divitiis, R. Petronzio, and L. Silvestrini, Nucl. Phys. **B504**, 45 (1997); G. Eilam *et al.*, Phys. Lett. B **510**, 227 (2001); X. L. Wang *et al.*, Phys. Rev. D **50**, 5781 (1994); R. D. Peccei and X. Zhang, Nucl. Phys. **B337**, 269 (1990); J. J. Cao *et al.*, Phys. Rev. D **75**, 075021 (2007); J. J. Liu, C. S. Li, L. L. Yang, and L. G. Jin, Phys. Lett. B **599**, 92 (2004).

[4] A. Cordero-Cid, M. A. Perez, G. Tavares-Velasco, and J. J. Toscano, Phys. Rev. D **70**, 074003 (2004); J. A. Aguilar-Saavedra, Acta Phys. Pol. B **35**, 2695 (2004); W. Wagner, Rep. Prog. Phys. **68**, 2409 (2005); J. M. Yang, Ann. Phys. (N.Y.) **316**, 529 (2005); E. Malkawi and C. P. Yuan, Phys. Rev. D **52**, 472 (1995); F. Larios, E. Malkawi, and C. P. Yuan, arXiv:hep-ph/9704288; O. J. P. Eboli, M. C. Gonzalez-Garcia, and S. F. Novaes, Phys. Lett. B **415**, 75 (1997); U. Baur, A. Juste, L. H. Orr, and D. Rainwater, Phys. Rev. D **71**, 054013 (2005); F. Larios, R. Martinez, and M. A. Perez, Phys. Rev. D **72**, 057504 (2005); T. Han, R. D. Peccei, and X. Zhang, Nucl. Phys. **B454**, 527 (1995); F. del Aguila, M. Perez-Victoria, and J. Santiago, Phys. Lett. B **492**, 98 (2000).

[5] W. Buchmuller and D. Wyler, Nucl. Phys. **B268**, 621 (1986).

[6] P. M. Ferreira and R. Santos, Proc. Sci., TOP2006 (2006) 004 [arXiv:hep-ph/0603131], and references therein.

[7] A. Ali and D. London, Eur. Phys. J. C **9**, 687 (1999); A. J. Buras, P. Gambino, M. Gorbahn, S. Jager, and L. Silvestrini, Phys. Lett. B **500**, 161 (2001); G. D'Ambrosio, G. F. Giudice, G. Isidori, and A. Strumia, Nucl. Phys. **B645**, 155 (2002).

[8] K. Agashe, M. Papucci, G. Perez, and D. Pirjol, arXiv: hep-ph/0509117.

[9] W. M. Yao *et al.* (Particle Data Group), J. Phys. G **33**, 1 (2006).

[10] A. Hocker, H. Lacker, S. Laplace, and F. Le Diberder, Eur. Phys. J. C **21**, 225 (2001); J. Charles *et al.*, Eur. Phys. J. C **41**, 1 (2005); updates at http://ckmfitter.in2p3.fr/.

[11] A. P. Heinson (CDF and D0 Collaborations), AIP Conf. Proc. **870**, 223 (2006).

[12] G. Buchalla, A. J. Buras, and M. E. Lautenbacher, Rev. Mod. Phys. **68**, 1125 (1996).

[13] G. Abbiendi *et al.* (OPAL Collaboration), Phys. Lett. B **521**, 181 (2001).

[14] S. Chekanov *et al.* (ZEUS Collaboration), Phys. Lett. B **559**, 153 (2003).

[15] F. Abe *et al.* (CDF Collaboration), Phys. Rev. Lett. **80**, 2525 (1998).

[16] A. Ali, E. Lunghi, C. Greub, and G. Hiller, Phys. Rev. D **66**, 034002 (2002); A. J. Buras, A. Czarnecki, M. Misiak, and J. Urban, Nucl. Phys. **B631**, 219 (2002).

[17] E. Barberio *et al.* (Heavy Flavor Averaging Group (HFAG)), arXiv:0704.3575; and updates at http://www.slac.stanford.edu/xorg/hfag/.

[18] B. Aubert *et al.* (*BABAR* Collaboration), Phys. Rev. Lett. **93**, 081802 (2004); M. Iwasaki *et al.* (Belle Collaboration), Phys. Rev. D **72**, 092005 (2005).

[19] K. S. M. Lee, Z. Ligeti, I. W. Stewart, and F. J. Tackmann, Phys. Rev. D **75**, 034016 (2007), and references therein.

[20] M. Okamoto *et al.*, Nucl. Phys. B, Proc. Suppl. **140**, 461 (2005); S. Hashimoto, A. S. Kronfeld, P. B. Mackenzie, S. M. Ryan, and J. N. Simone, Phys. Rev. D **66**, 014503 (2002).

[21] A. V. Manohar and M. B. Wise, Cambridge Monogr. Part. Phys., Nucl. Phys., Cosmol. **10**, 1 (2000).

[22] N. Isgur and M. B. Wise, Phys. Lett. B **232**, 113 (1989); **237**, 527 (1990).
[23] W. D. Goldberger, arXiv:hep-ph/9902311; B. M. Dassinger, R. Feger, and T. Mannel, Phys. Rev. D **75**, 095007 (2007).
[24] B. Grinstein and Z. Ligeti, Phys. Lett. B **526**, 345 (2002); **601**, 236(E) (2004).
[25] B. Aubert *et al.* (*BABAR* Collaboration), arXiv:hep-ex/0607076.
[26] M. Gremm, A. Kapustin, Z. Ligeti, and M. B. Wise, Phys. Rev. Lett. **77**, 20 (1996); M. B. Voloshin, Phys. Rev. D **51**, 4934 (1995).
[27] B. Aubert *et al.* (*BABAR* Collaboration), Phys. Rev. D **69**, 111104 (2004).
[28] P. Urquijo (private communication).
[29] P. Urquijo *et al.* (Belle Collaboration), Phys. Rev. D **75**, 032001 (2007).
[30] M. C. Arnesen, B. Grinstein, I. Z. Rothstein, and I. W. Stewart, Phys. Rev. Lett. **95**, 071802 (2005).
[31] M. Okamoto *et al.*, Nucl. Phys. B, Proc. Suppl. **140**, 461 (2005).
[32] J. Shigemitsu *et al.*, Nucl. Phys. B, Proc. Suppl. **140**, 464 (2005).
[33] C. W. Bauer, Z. Ligeti, and M. E. Luke, Phys. Rev. D **64**, 113004 (2001); Phys. Lett. B **479**, 395 (2000).
[34] H. Kakuno *et al.* (Belle Collaboration), Phys. Rev. Lett. **92**, 101801 (2004); I. Bizjak *et al.* (Belle Collaboration), Phys. Rev. Lett. **95**, 241801 (2005); B. Aubert *et al.* (*BABAR* Collaboration), arXiv;hep-ex/0507017.
[35] K. Abe *et al.* (Belle Collaboration), Phys. Rev. Lett. **96**, 221601 (2006); B. Aubert *et al.* (*BABAR* Collaboration), Phys. Rev. Lett. **98**, 151802 (2007).
[36] P. Ball, G. W. Jones, and R. Zwicky, Phys. Rev. D **75**, 054004 (2007), and references therein.
[37] CDF Collaboration, http://www-cdf.fnal.gov/physics/new/bottom/060316.blessed-bsmumu3.
[38] Z. Ligeti, Int. J. Mod. Phys. A **20**, 5105 (2005); M. Bona *et al.* (UTfit Collaboration), J. High Energy Phys. 03 (2006) 080; F. J. Botella, G. C. Branco, M. Nebot, and M. N. Rebelo, Nucl. Phys. **B725**, 155 (2005).
[39] Z. Ligeti, M. Papucci, and G. Perez, Phys. Rev. Lett. **97**, 101801 (2006); Y. Grossman, Y. Nir, and G. Raz, Phys. Rev. Lett. **97**, 151801 (2006); M. Blanke, A. J. Buras, D. Guadagnoli, and C. Tarantino, J. High Energy Phys. 10 (2006) 003.
[40] K. Agashe, A. Belyaev, T. Krupovnickas, G. Perez, and J. Virzi, Phys. Rev. D **77**, 015003 (2008).
[41] K. Agashe, G. Perez, and A. Soni, Phys. Rev. D **75**, 015002 (2007); G. F. Giudice, C. Grojean, A. Pomarol, and R. Rattazzi, J. High Energy Phys. 06 (2007) 045.